THE JOURNAL OF BIOLOGICAL CHEMISTRY VOL. 290, NO. 16, pp. 10038–10044, April 17, 2015


# Conformational Changes Leading to T7 DNA Delivery upon Interaction with the Bacterial Receptor*

Received for publication, September 24, 2014, and in revised form, February 13, 2015 Published, JBC Papers in Press, February 19, 2015, DOI 10.1074/jbc.M114.614222

**Verónica A. González-García[‡], Mar Pulido-Cid[‡], Carmela Garcia-Doval[‡], Rebeca Bocanegra[‡], Mark J. van Raaij[‡], Jaime Martín-Benito[‡], Ana Cuervo[‡1], and José L. Carrascosa[‡§2]**

*From the [‡]Structure of Macromolecules Department, Centro Nacional de Biotecnología (CSIC), Darwin 3, Cantoblanco, 28049 Madrid and [§]Instituto Madrileño de Estudios Avanzados en Nanociencia (IMDEA Nanociencia), Cantoblanco, 28049 Madrid, Spain*

**Background:** T7 bacteriophage infects *E. coli* bacteria; during this process, the tail recognizes the bacterial receptor.
**Results:** Interactions of T7 with rough LPS trigger DNA delivery by promoting changes in the tail tube.
**Conclusion:** *E. coli* rough LPS act as the receptor *in vitro* for T7 bacteriophage.
**Significance:** Biotechnological application of bacteriophages as antibacterial agents demands detailed molecular knowledge of bacteriophage infection.

**The majority of bacteriophages protect their genetic material by packaging the nucleic acid in concentric layers to an almost crystalline concentration inside protein shells (capsid). This highly condensed genome also has to be efficiently injected into the host bacterium in a process named ejection. Most phages use a specialized complex (often a tail) to deliver the genome without disrupting cell integrity. Bacteriophage T7 belongs to the *Podoviridae* family and has a short, non-contractile tail formed by a tubular structure surrounded by fibers. Here we characterize the kinetics and structure of bacteriophage T7 DNA delivery process. We show that T7 recognizes lipopolysaccharides (LPS) from *Escherichia coli* rough strains through the fibers. Rough LPS acts as the main phage receptor and drives DNA ejection *in vitro*. The structural characterization of the phage tail after ejection using cryo-electron microscopy (cryo-EM) and single particle reconstruction methods revealed the major conformational changes needed for DNA delivery at low resolution. Interaction with the receptor causes fiber tilting and opening of the internal tail channel by untwisting the nozzle domain, allowing release of DNA and probably of the internal head proteins.**

Bacteriophages depend on their bacterial host for production of new viral particles. Unlike eukaryotic viruses, most bacterial viruses translocate their genetic material into the host cytoplasm, whereas the empty capsid remains on the bacterial surface (1–3). Transport of the polyanionic genome through the bacterial membranes implicates overcoming several barriers including membrane impermeability to nucleic acids and degradation by periplasmic nucleases (4). Non-tailed phages use bacterial complexes to translocate their genome (5), or they use proteins (6) or membranes (7) to form new tubular structures. The most common strategy for internalizing the bacteriophage genome is via a specialized tail complex (2, 4, 8, 9) attached through the connector protein to the capsid at the DNA packaging vertex. This complex has several functions that govern the sequence of events necessary for efficient transfer of the genetic material into the host (10, 11). The tail first closes the connector channel, preventing DNA leakage from the capsid after packaging. During infection, the tail specifically recognizes the bacterial receptor and transmits the gate-opening signal for DNA delivery. Finally, the tail conduit protects the genome during transfer to allow it to reach the bacterial cytoplasm safely.

Bacteriophage T7 belongs to the *Podoviridae* family; its tail is an ~2.7-MDa macromolecular complex. At least four proteins (gp8, gp11, gp12, and gp17) make up the T7 tail, which forms a central tubular structure with a closed, twisted nozzle at the bottom formed by a gp12 hexamer. This tubular assembly is surrounded by six protruding fibers specializing in receptor recognition, each of which is a gp17 trimer (12, 13). Both proteins are docked to the connector (gp8) by a dodecameric ring termed adaptor or gatekeeper (gp11). Comparative structural studies of bacteriophage tail before and after DNA ejection have been previously reported for phages $\phi$29 (14), SPP1 (15), and T4 (16). The mechanism of DNA transport is probably best studied for T4, where the contraction of the sheath drives the tail tube trough the outer membrane, forming a channel. In the case of T7, the tail is not long enough to puncture the bacterial envelope. Thus, it is postulated that some *Podoviridae* adopt a strategy similar to non-tailed viruses and enlarge their tail conduit by forming a new proteinaceous tubular structure when they infect Gram-negative hosts (11, 17, 18). Using cryo-electron tomography, Hu *et al.* visualized a temporary extension of the T7 tail during infection (18); they suggest that this extension is formed by the T7 core proteins gp14, gp15, and gp16. As these proteins are found inside the mature virus capsid, they could only form a conduit for DNA protection after transport through the tail channel and reassembly in the bacterial envelope (11, 18). The molecular mechanisms that control channel

* This work was supported by the Spanish Ministry of Economy and Competitiveness Grants BFU2011-29038 (to J. L. C.), BFU2011-25090 (to J. M.-B.), and BFU2011-24843 (to M. J. v. R.).
The three-dimensional EM volume has been deposited in the EM Data Base (http://www.ebi.ac.uk/pdbe/emdb/) with accession number EMD-2717.
[1] To whom correspondence may be addressed: Centro Nacional de Biotecnología, CSIC. c/ Darwin 3, Cantoblanco, 28049 Madrid, Spain. Tel.: 34-915854509; Fax: 34-915854506; E-mail: acuervo@cnb.csic.es.
[2] To whom correspondence may be addressed: Centro Nacional de Biotecnología, CSIC. c/ Darwin 3, Cantoblanco, 28049 Madrid, Spain. Tel.: 34-915854509; Fax: 34-915854506; E-mail: jlcarras@cnb.csic.es.

opening and the precise conformational changes in the tail during this process are nonetheless unknown.

The Gram-negative bacterial envelope is composed of a peptidoglycan layer surrounded by two membranes (9, 19). During infection, the phage is thought to interact first with a surface molecule that allows correct tail orientation relative to the bacterial envelope, followed by an irreversible interaction with the same or a different receptor; this second interaction is needed to trigger opening of the tail channel (20). Viruses that infect Gram-negative bacteria, such as *Escherichia*, *Salmonella*, *Shigella*, or *Yersinia* genus, often use lipopolysaccharide (LPS)[3] as a receptor, assisted by porins or outer membrane proteins (21–23). In the case of phage T7, the identity of the bacterial receptor that triggers the conformational changes in the tail is debated. In the late 1960s, LPS from *Escherichia coli* B was reported to neutralize T7 (24). A few years later, Lindberg (21) claimed that T7 phages only infect rough strains of *E. coli* and *Shigella*, corroborating the importance of LPS in the infection mechanism. The tendency in the early 2000s was to consider LPS only a primary phage T7 receptor that mediates reversible binding to the bacterial surface, whereas another secondary receptor was suggested to be necessary for irreversible binding and infection (20, 25).

Here we used biochemical approaches to characterize the T7 particle interaction with purified LPS from *E. coli* rough strains. These studies allowed us to establish an *in vitro* ejection system for bacteriophage T7 and to carry out structural studies of the bacteriophage after ejection. Altogether these findings give new clues about the conformational changes needed in the tail to allow T7 genome transfer from the phage capsid into the bacterial cytoplasm.

## EXPERIMENTAL PROCEDURES

*DNA Ejection Assays*—T7 ($10^{11}$ pfu/ml) was incubated with 250 $\mu$g/ml LPS from the rough *E. coli* EH100 Ra mutant (Sigma-Aldrich) at 37 °C; aliquots were collected at 0, 15, 30, 60, 90, and 180 min, diluted in TMS (50 mM Tris-HCl pH 7.8, 10 mM $MgCl_2$, 100 mM NaCl), and stored on ice. Samples were then mixed with BL21 *E. coli* bacteria, plated on soft agar, and incubated (overnight, 37 °C) to determine viral titer. DNase protection assays were performed as described (26). For the reactions, the same T7/LPS ratio was incubated (37 °C) for the times indicated above.

*LPS Binding Assays*—For virus interaction assays, T7 ($10^{11}$ pfu/ml) was incubated with 250 $\mu$g/ml rough LPS from *E. coli* EH100 Ra mutant or smooth LPS from *E. coli* 0111:B4 (Sigma-Aldrich) (3 h, 37 °C). We incubated ~0.1 mg/ml recombinant tail complex, alone or with gp17 purified as described (13, 27), with 250 $\mu$g/ml rough LPS (2 h, 30 °C). Samples were loaded on glow-discharged copper grids covered with a thin carbon layer; negatively stained with 2% (w/v) phosphotungstic acid or uranyl acetate; and observed by EM.

*Fluorescence DNA Ejection Assays*—Fluorescence signal was recorded in a fluorimeter (Hitachi F-7000) operated at 491- and 509-nm wavelengths for excitation and emission, respectively. T7 particles (~$5 \times 10^9$ pfu) were incubated with 0.7 $\mu$M Yo-Yo fluorophore (Invitrogen) at 37 °C for ~1000 s until the signal stabilized. Rough LPS from EH100 Ra mutant (Sigma-Aldrich) was added at 10, 20, 50, and 100 $\mu$g/ml, and the signal was recorded for at least 3000 s. As LPS forms big aggregates in solution, to calculate $K_{bind}$ constants, the molecular mass of the LPS was estimated to 10 kDa per chain (28). As a control, the experiment was repeated adding TMS or 10 $\mu$g/ml smooth LPS from *E. coli* 0111:B4 (Sigma-Aldrich). Curves were normalized and fitted to the double exponential equation (Equation 1) by Andres *et al.* (28) using the KaleidaGraph program (Synergy Software)

$$\mathrm{DNA}\,(t) = A_0 \times (1 - (1/k_{open} - k')(k_{open} \times e^{(-k' \times t)} - k' \times e^{(-k_{open} \times t)}) \quad \text{(Eq. 1)}$$

where $k' = C_{LPS} \times k_{bind}$. The $k_{open}$ constant was calculated after fitting the data to a monoexponential curve at LPS saturating concentrations (50 and 100 $\mu$g/ml).

*Electron Microscopy and Image Processing*—The T7-LPS ejection reaction samples were incubated (3 h, 37 °C), applied to Quantifoil 2-$\mu$m holey carbon grids coated with a thin carbon layer, frozen in liquid ethane, and transferred to a Tecnai G20 FEG200 electron microscope (FEI) operated as described (13) at ×10,8696 magnification and 1.5–3.5-$\mu$m defocus range. Micrographs were contrast transfer function-corrected using standard XMIPP software (29); particles were manually selected with XMIPP (30) and downsampled to a factor of 4 to a final pixel size ratio of 5.5 Å/pixel. Images were classified using XMIPP reference-free clustering approach classification methods (CL2D) (31). A filtered volume of the T7 tail (32) was used as the initial model, and 1050 particles corresponding to side views were used to generate an initial three-dimensional model based on the common lines method implemented in EMAN software (33) using a restricted angle projection protocol and applying 6-fold symmetry. A final model was obtained using the XMIPP Projection Matching package (29, 34). To determine volume resolution, the particles were divided into two independent datasets (gold standard) and reprocessed. The resolution of the final reconstruction was estimated to ~20 Å. The three-dimensional model was deposited in the Electron Microscopy Data Bank (EMDB) (accession number EMD-2717). The three-dimensional reconstruction images were generated using Chimera (35).

## RESULTS

*T7 Ejects Its DNA Genome in Vitro in the Presence of Rough LPS*—It has been postulated that *E. coli* rough LPS could act as the receptor for bacteriophage T7 (21, 36). To test this hypothesis, we incubated T7 phages with rough LPS. This incubation led to inactivation of the virions (Fig. 1*A*). After 30 min, nearly half the particles were inactivated; this percentage increased to >90% after 90 min. We used DNase protection assays to test the effect of rough LPS on T7 particles and found a decrease in the amount of DNA protected within the capsids (Fig. 1*B*). This finding suggested that the decrease in the percentage of infective viral particles was the result of rough LPS-induced DNA ejection. Densitometry analysis of protected DNA as a function

[3] The abbreviations used are: LPS, lipopolysaccharide(s); cryo-EM, cryo-electron microscopy.

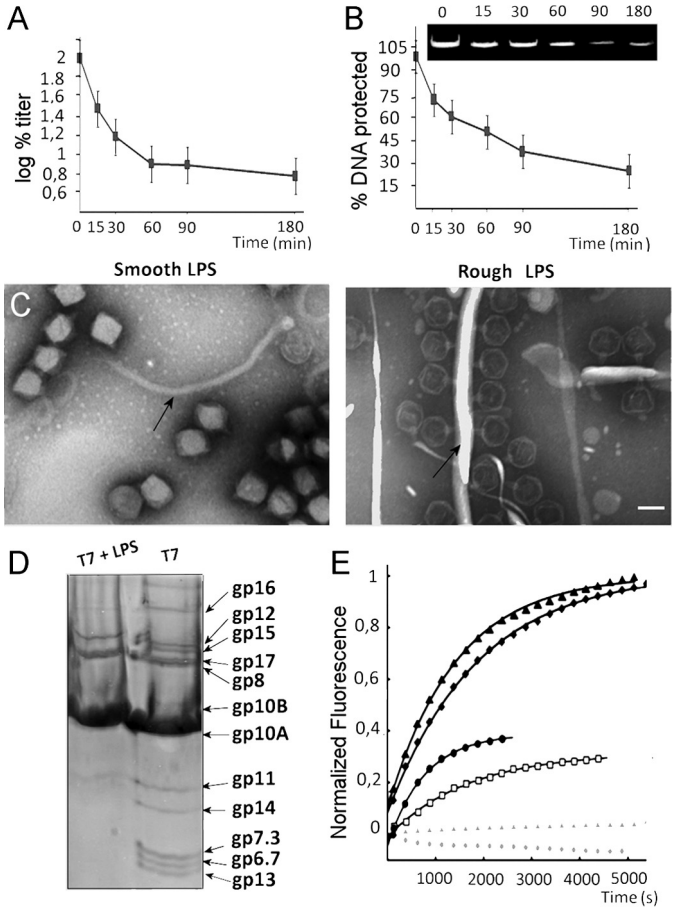


FIGURE 1. **Rough LPS triggers T7 phage genome ejection *in vitro*.** *A*, T7 particles ($10^{11}$ pfu/ml) were incubated with ~250 μg/ml rough LPS at 37 °C for the indicated times and plated. The log of the percentage of titer is plotted. *Error bars* indicate mean ± S.D. *B*, deprotection of genomic DNA from DNase digestion after incubation of T7 particles with rough LPS. The *inset* shows the ethidium bromide-stained 0.8% agarose gel from which the densitometric analysis shown in the graph was obtained. *Error bars* indicate mean ± S.D. *C*, electron micrographs showing negatively stained particles incubated with smooth LPS (*left*) or rough LPS (*right*). *Arrows* indicate the LPS layers. *Bar* = 50 nm. *D*, denaturing gel electrophoresis of T7 phages before (*right*) and after (*left*) incubation with rough LPS. *E*, DNA ejection of T7 phages (~$5 \times 10^9$ pfu) monitored by fluorescence at 37 °C in the presence of Yo-Yo fluorescent dye. DNA release was triggered by the addition of rough LPS: 10 μg/ml (*open black squares*), 20 μg/ml (*closed black circles*), 50 μg/ml (*closed black squares*), and 100 μg/ml (*closed black triangles*). Lines show overall fit of the data to the equation corresponding to two first order reactions (25). The control experiment was performed without LPS (*closed gray triangles*) or with smooth LPS (*closed gray circles*). For clarity, only 1 out of 20 data points has been represented.

of incubation time (Fig. 1*B*, *inset*) showed a reduction that is consistent with the drop of phage titer (Fig. 1*A*). DNA ejection *in vitro* in the presence of rough LPS was confirmed by EM experiments, in which negatively stained T7 particles were incubated with LPS from rough or smooth (negative control) *E. coli* strains (Fig. 1*C*). As predicted, no phages bound to the smooth LPS and no staining agent penetrated the heads, indicating that the virus remained DNA-filled (Fig. 1*C*, *left*). In contrast, incubation with LPS from rough strain *E. coli* showed T7 particle attachment to rough LPS layers, and the staining agent penetrated the capsid, indicating that DNA had been ejected (Fig. 1*C*, *right*).

These experiments demonstrated that incubation with rough LPS is sufficient to trigger DNA ejection *in vitro* and allowed us to establish an *in vitro* system to study T7 genome delivery. Similar findings have been reported previously for P22 (37). In our experiments with T7 bacteriophage, no proteins were observed inside the capsid after ejection (Fig. 1*C*, *right*), suggesting that the core proteins were also ejected (18). Also, we did not observe the core complex attached to the tail structure (Fig. 1*C*, *right*) as it disassembles rapidly after DNA ejection (18). Electrophoretic analysis of the ejection reaction components showed that neither the core proteins (gp14, gp15, and gp16), nor proteins gp6.7, gp7.3, and gp13 were present after DNA ejection, suggesting that they are proteolyzed after DNA translocation (Fig. 1*D*). Similar results have been reported *in vivo* (38), which implies that this degradation is essential for the infection mechanism, possibly to avoid the long-term presence of a membrane channel, which would affect cell integrity after DNA transfer to the cytoplasm. Degradation of these proteins in the *in vitro* reactions also suggests that one of the viral proteins might proteolyze this structure.

To follow real-time DNA ejection at 37 °C, we performed a fluorescence experiment using the Yo-Yo fluorescent DNA binding dye. The fluorescent signal increased immediately after the addition of rough strain LPS receptor to the sample. After 1000 s, ~50% of viruses had ejected their genome and the curve stabilized in a plateau at ~5000 s (Fig. 1*E*). The addition of DNase led to a decrease in the fluorescence signal (data not shown). The signal was dependent on rough LPS addition as DNA was not released when LPS was not present nor when smooth strain LPS was added (Fig. 1*E*, *gray symbols*). The fluorescence intensity increase was also dependent on rough strain LPS concentration until saturation was reached at ~50 μg/ml, when $5 \times 10^9$ pfu of virus was used. We observed no further increase in fluorescence values when the virus was incubated with ~100 μg/ml rough LPS (Fig. 1*E*, *black triangles*). As for T5 and P22 (28, 39), T7 DNA ejection can be fitted to two first order reactions defined by two constants: 1) the first constant describes virus-receptor interaction (defined by $k_{bind}$), and 2) the second constant describes the channel opening reaction (defined by $k_{open}$). Virus-receptor interaction is LPS concentration-dependent. The data fit well to the equation proposed by Andres *et al.* (28). As in their case, estimation of LPS aggregates to a molecular mass of 10 kDa per chain allowed us to calculate $k_{bind}$ (28). We obtained a $k_{bind}$ value of ~$10^4\ M^{-1}\ s^{-1}$. Fitting of the data at saturating LPS concentrations to a monoexponential equation gave a $k_{open}$ value of ~$4.2 \times 10^{-4}\ s^{-1}$, in the same order of magnitude as reported for podovirus P22 ($k_{open}$ ~$4.5 \times 10^{-4}\ s^{-1}$) (28). The slower *Podoviridae* kinetics as compared with *Siphoviridae* (28, 39) might be due to ejection of internal head proteins as well as DNA.

The C-terminal portion of the fiber protein (gp17) is considered essential for virus-receptor interaction (12). To determine the structural component that interacts with rough LPS, we incubated rough LPS with recombinant fiber-less tail complexes and with fiber-containing tail complexes (13). EM images of the negatively stained fiber-containing samples showed the tail complex attached to the rough LPS, presumably through the fibers (Fig. 2, *A* (*left*), and *B*, *arrows*), whereas no tail complexes were attached to rough LPS in the absence of fibers (Fig. 2*A*, *right*, *circles*). Aggregation of rough LPS in samples

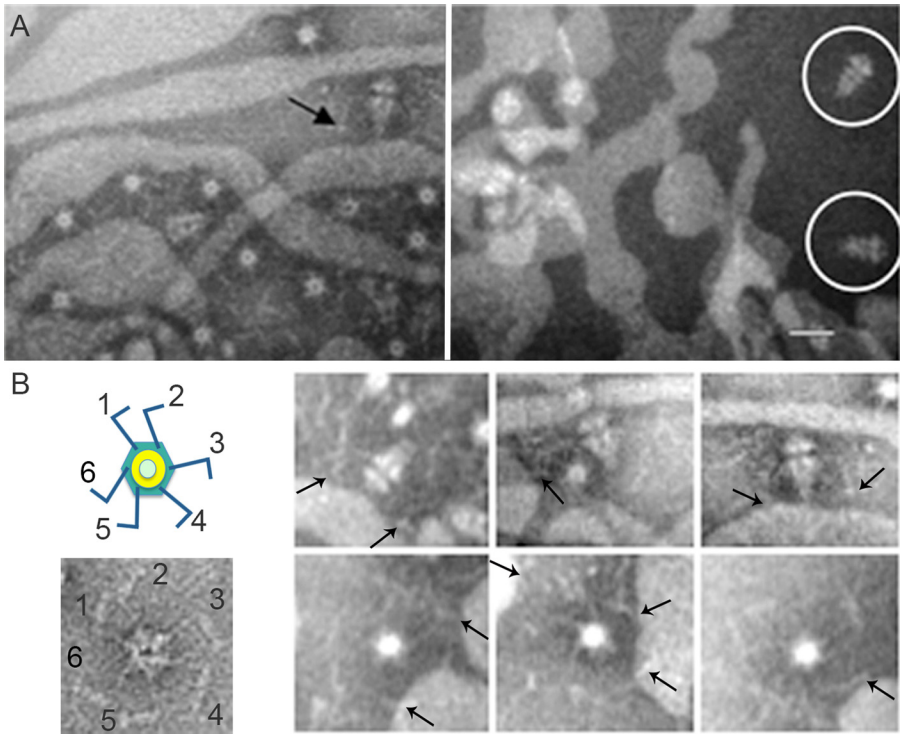


FIGURE 2. **T7 bacteriophage interacts with rough LPS trough the fiber protein.** *A*, electron micrographs showing negatively stained fibered (*left*) or fiber-less tail complexes (*right*) incubated with LPS. The *arrow* indicates representative tail complex showing interaction between the fiber and rough LPS; a *white circle* surrounds non-fibered complexes. *Bar* = 30 nm. *B*, *left*, uranyl acetate negatively stained end-on view tail complex where the six protruding fibers were labeled. The scheme on the *top* represents a tail complex where the tubular structure has been colored in *green* (tail proteins) and *yellow* (connector), and the fibers have been colored in *blue*. *Right*, gallery showing different tail complexes in end-on and side views interacting with the LPS. *Arrows* point to representative fiber complexes.

with fiber complexes could be due to interaction of each of the six fibers with a different LPS layer (Fig. 2, *A* (*left*) and *B*). The results imply that T7 bacteriophage interacts with its receptor through the fibers and that this interaction triggers the conformational changes that lead to DNA delivery.

*Structural Characterization of T7 DNA Delivery—In vitro* ejection samples consisting of T7 and rough strain LPS were incubated (3 h, 37 °C) and then vitrified in ethane. Cryo-EM images showed a double-layered LPS filament with viruses attached through the tail complex (Fig. 3*A*). Incubation of T7 phages with rough LPS led to delivery of the genome and the internal core proteins; as mentioned above, we did not observe core proteins in the capsid after genome ejection reactions. Two-dimensional averages belonging to different side view classes showed the characteristic conical shape of the tail structure, with a central channel that runs from the connector structure to the LPS (Fig. 3*B*). The two-dimensional classes correlated well with the individual particles (Fig. 3*B*). We obtained the three-dimensional structure of the tail complex in the post-ejected conformation by image processing of cryo-EM data at ~20 Å (Fig. 3*C*). Based on the T7 tail complex structure (13), we segmented the density corresponding to the tail proteins (connector, gp8; gatekeeper, gp11; nozzle, gp12; and fibers, gp17) out of the volume, as well as the capsid protein (gp10) (Fig. 3*C*). We observed the characteristic shape of the connector structure, embedded in the viral capsid, as well as the N-terminal domains of the six protruding fibers attached to the conical structure and running perpendicular to the central channel (Fig. 3*C*). Although denaturing gel electrophoresis of the ejection reaction samples demonstrated that the gp17 protein is not degraded during the process (Fig. 1*D*), we were not able to see the C-terminal domain of gp17 interacting with the LPS in our reconstruction, probably due to the flexibility of the fiber structure. The nozzle complex is found at the opposite side of the connector, ending in an open channel with a 40 Å overall diameter, large enough to permit passage of the dsDNA viral genome.

Comparison of pre- and post-DNA ejection conformations (Fig. 4, *A* and *B*) permitted the definition of the conformational changes in the tail structure that correlate with DNA delivery. Some of these changes were defined using cryo-electron tomography by Hu *et al.* (18), who identified a change in fiber orientation. In the mature virus, the fibers are attached to the head and undergo considerable conformational change from an upward to a downward conformation, which allows interaction with the bacterial envelope (18). Although fiber flexibility did not allow us to visualize its C-terminal portion interacting with the rough LPS, single-particle reconstruction methods allowed us to increase resolution of the tail reconstruction, and thus to define more accurately the changes in the gp17 fiber N-terminal domain. After LPS interaction, the N-terminal fiber domain tilts by ~30° (Fig. 4, *B* and *C*), allowing the C-terminal domain to contact the rough LPS layer. The gp17 N-terminal domain attaches to the tubular structure through a three-lobule region (13) that could act as a hinge, allowing the long fiber structure to tilt. This change in surface contact between fiber and tubular structure might act as a sensor to trigger opening of the tail. Indeed, the DNA halted precisely at this point in

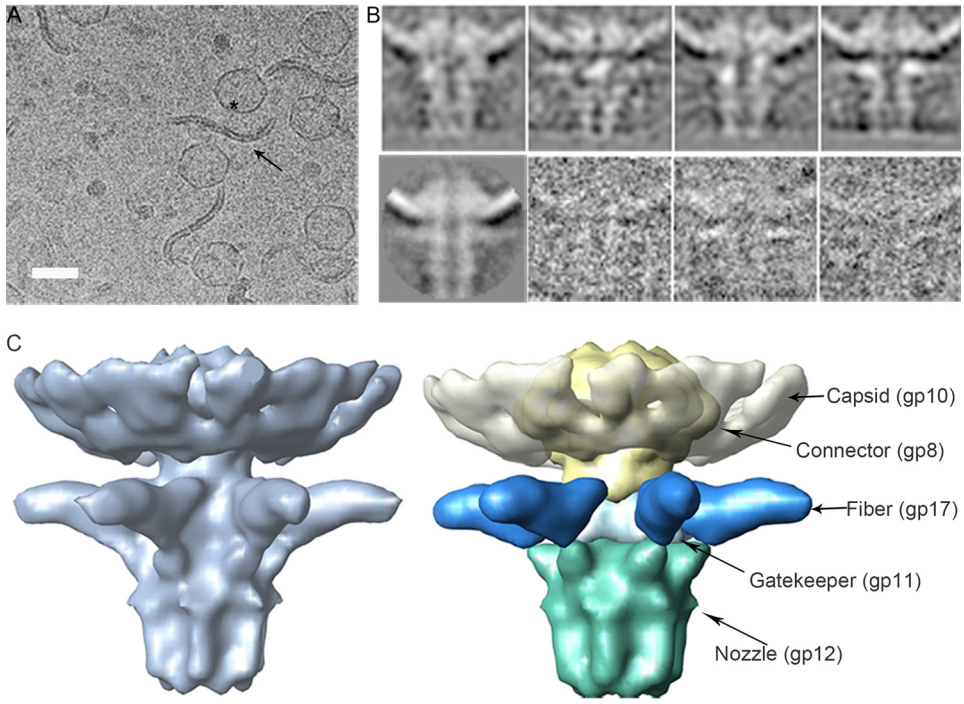


FIGURE 3. **Structural characterization of T7 tail after interaction with rough LPS.** *A*, a representative field of a cryo-EM micrograph showing T7 phages after the ejection reaction. The *arrow* indicates an LPS layer, and the *asterisk* indicates an empty virus. *Bar* = 50 nm. *B*, *top*, two-dimensional classes corresponding to different side views. *Bottom*, two-dimensional average and three individual particles. *C*, *left*, side view of the three-dimensional model showing the tail after DNA ejection. *Right*, segmentation of the volumes corresponding to the proteins present in the complex. *Arrows* indicate the location of proteins gp8 (*yellow*), gp10 (*white*), gp11 (*light blue*), gp12 (green), and N-terminal gp17 (*dark blue*) segmented in the complex.

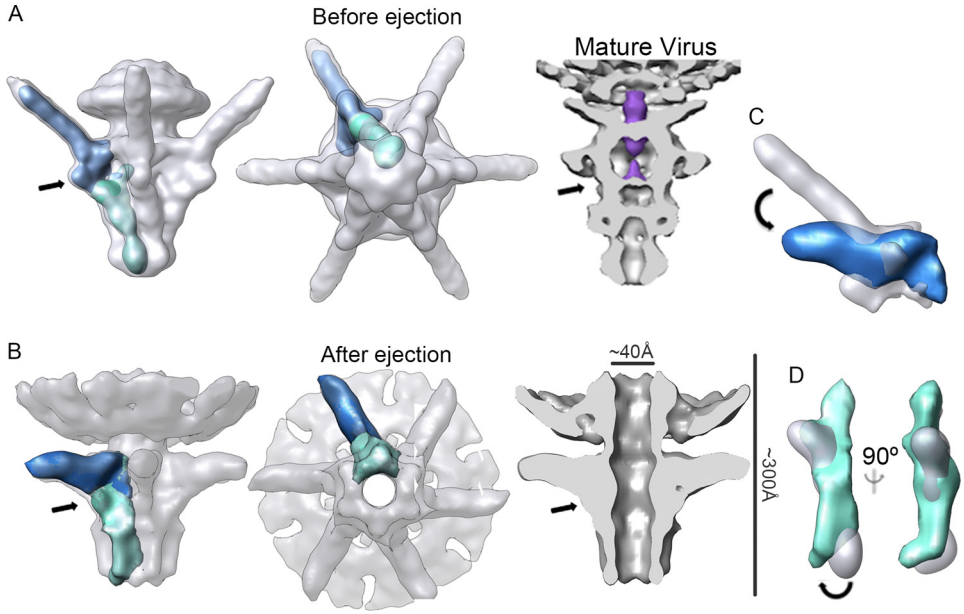


FIGURE 4. **Conformational changes in the tail complex after DNA ejection.** *A*, three-dimensional reconstruction of the T7 tail before DNA ejection (EMD-5689) (13) in a side view (*left*) and an end-on view (*middle*). *Right*, a section view of the tail segmented from the mature virus (EMD-1163) (32); DNA inside the channel is shown in *purple*. *B*, three-dimensional reconstruction of the T7 tail after DNA ejection in side (*left*), end-on (*middle*), and section views (*right*). *Arrows* indicate the interaction between the fiber and the gatekeeper and the position where the DNA appears to be halted. The length of the complex and the dimension of the channel diameter are indicated. A single subunit of the gp12 protein (nozzle) and a trimer of N-terminal gp17 fiber domain are shown in *green* and *dark blue*, respectively. *C*, overlap of the gp17 trimer before (*white*) and after (*blue*) DNA ejection. An *arrow* shows predicted movement of the fiber. *D*, overlap of a gp12 monomer before (*white*) and after (*green*) DNA ejection; two views of the same segmented electron density are shown. An *arrow* indicates the predicted movement of the nozzle.

the gatekeeper/adaptor channel (Fig. 4*A*, *arrow*), suggesting that there is a valve that retains the DNA. Long-tailed viruses have a gatekeeper valve (40), and other *Podoviridae* phages share the T7 DNA topology, which suggests that they use the same mechanism to secure the genome (41–43). The second major conformational change that can be observed at this resolution consists of the opening of the ejection channel by untwisting of the tail nozzle domain (compare Fig. 4, *A* and *B*).

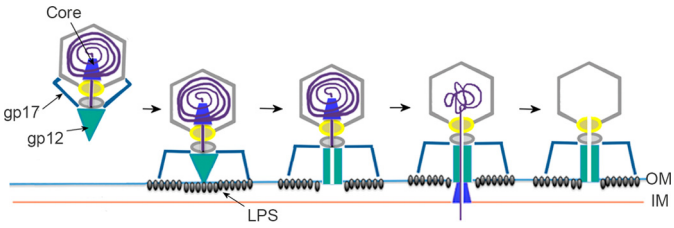


FIGURE 5. **Scheme of the proposed initial steps of T7 infection.** The main components in this process (nozzle, gp12; fiber, gp17; and LPS) are labeled. Synchronized interaction of the six fibers with the rough LPS assists correct orientation of the tail and triggers opening of the valve, liberating DNA. As a result, the nozzle changes its conformation, opening the channel to allow translocation and subsequent assembly of the core in the bacterial envelope; this generates the conduit for safe DNA delivery into the cytoplasm, after which the core complex is degraded.

The gp12 monomer is composed of three domains that form a shoulder and two lobes (13). Overlapping the segmented monomers from pre- and post-ejected conformations showed an ~10° shift around the longitudinal axis of the gp12 apical lobe domain (Fig. 4*D*). Channel opening is thus the result of a concerted movement by the six gp12 monomers. The structural similarity of the T7 nozzle structure with those of other *Podoviridae* such as P-SSP7, K1E, and ϵ15 (44) suggests that these viruses could share the same tail-opening mechanism.

## DISCUSSION

Increased bacterial resistance to antibiotics has revived interest in using bacteriophages as antibacterial agents. Correct implementation of such treatments demands detailed molecular knowledge of bacteriophage infection. Based on these results, we describe the initial steps of T7 infection (Fig. 5). In this model, a series of conformational changes is triggered sequentially. The first interaction of the virus with the outer membrane remains elusive, but studies on bacteriophages belonging to the *Podoviridae* family suggest that membrane proteins (probably porins) may be involved (22, 23). This first interaction could be essential to facilitate subsequent recognition of the rough LPS viral receptor. Then, binding of the C-terminal gp17 fiber protein to a component of the rough strain LPS chain (probably a heptose (45)) would force tilting of the N-terminal fiber docking point, altering the fiber-gatekeeper interface. Our hypothesis is that these modifications at the fiber-gatekeeper interface could trigger the conformational changes in the nozzle, leading to the opening of the ejection channel and thus leading to the DNA release. The force of the liberated DNA could then untwist the tail nozzle, forcing the irreversible structural modification needed to open the ejection channel. The channel is large enough to transport the DNA and the unfolded core proteins (46), which degrade the peptidoglycan layer and form a conduit to reach the bacterial cytoplasm. To avoid disrupting bacterial integrity, this membrane-spanning tube would disassemble and be degraded shortly after DNA transport.

*Acknowledgments—We thank José J. Fernández for support and advice with image processing and Rocío Arranz for technical support and help with cryo-EM image acquisition. We are indebted to Begoña Sot for help in fluorescence kinetics analysis and Catherine Mark for editorial assistance.*

## REFERENCES

1. Cuervo, A., Daudén, M. I., and Carrascosa, J. L. (2013) Nucleic acid packaging in viruses. *Subcell. Biochem.* **68,** 361–394
2. Molineux, I. J., and Panja, D. (2013) Popping the cork: mechanisms of phage genome ejection. *Nat. Rev. Microbiol.* **11,** 194–204
3. Hershey, A. D., and Chase, M. (1952) Independent functions of viral protein and nucleic acid in growth of bacteriophage. *J. Gen. Physiol.* **36,** 39–56
4. Bertin, A., de Frutos, M., and Letellier, L. (2011) Bacteriophage-host interactions leading to genome internalization. *Curr. Opin. Microbiol.* **14,** 492–496
5. Rakonjac, J., Bennett, N. J., Spagnuolo, J., Gagic, D., and Russel, M. (2011) Filamentous bacteriophage: biology, phage display and nanotechnology applications. *Curr. Issues Mol. Biol.* **13,** 51–76
6. Sun, L., Young, L. N., Zhang, X., Boudko, S. P., Fokine, A., Zbornik, E., Roznowski, A. P., Molineux, I. J., Rossmann, M. G., and Fane, B. A. (2014) Icosahedral bacteriophage ϕX174 forms a tail for DNA transport during infection. *Nature* **505,** 432–435
7. Peralta, B., Gil-Carton, D., Castaño-Díez, D., Bertin, A., Boulogne, C., Oksanen, H. M., Bamford, D. H., and Abrescia, N. G. (2013) Mechanism of membranous tunnelling nanotube formation in viral genome delivery. *PLoS Biol.* **11,** e1001667
8. Veesler, D., and Cambillau, C. (2011) A common evolutionary origin for tailed-bacteriophage functional modules and bacterial machineries. *Microbiol. Mol. Biol. Rev.* **75,** 423–433
9. Vinga, I., Sao-José, C., Tavares, P., and Santos, M. (2006) Bacteriophage entry in the host cell. in *Modern Bacteriophage Biology and Biotechnology*, (Wegrzyn, G., ed) pp. 167–170, Research Signpost, Kerala, India
10. Cuervo, A., and Carrascosa, J. L. (2012) Viral connectors for DNA encapsulation. *Curr. Opin. Biotechnol.* **23,** 529–536
11. Bhardwaj, A., Olia, A. S., and Cingolani, G. (2014) Architecture of viral genome-delivery molecular machines. *Curr. Opin. Struct. Biol.* **25,** 1–8
12. Garcia-Doval, C., and van Raaij, M. J. (2012) Structure of the receptor-binding carboxy-terminal domain of bacteriophage T7 tail fibers. *Proc. Natl. Acad. Sci. U.S.A.* **109,** 9390–9395
13. Cuervo, A., Pulido-Cid, M., Chagoyen, M., Arranz, R., González-García, V. A., Garcia-Doval, C., Castón, J. R., Valpuesta, J. M., van Raaij, M. J., Martín-Benito, J., and Carrascosa, J. L. (2013) Structural characterization of the bacteriophage T7 tail machinery. *J. Biol. Chem.* **288,** 26290–26299
14. Xiang, Y., Morais, M. C., Battisti, A. J., Grimes, S., Jardine, P. J., Anderson, D. L., and Rossmann, M. G. (2006) Structural changes of bacteriophage ϕ29 upon DNA packaging and release. *EMBO J.* **25,** 5229–5239
15. Plisson, C., White, H. E., Auzat, I., Zafarani, A., São-José, C., Lhuillier, S., Tavares, P., and Orlova, E. V. (2007) Structure of bacteriophage SPP1 tail reveals trigger for DNA ejection. *EMBO J.* **26,** 3720–3728
16. Kostyuchenko, V. A., Chipman, P. R., Leiman, P. G., Arisaka, F., Mesyanzhinov, V. V., and Rossmann, M. G. (2005) The tail structure of bacteriophage T4 and its mechanism of contraction. *Nat. Struct. Mol. Biol.* **12,** 810–813
17. Chang, J. T., Schmid, M. F., Haase-Pettingell, C., Weigele, P. R., King, J. A., and Chiu, W. (2010) Visualizing the structural changes of bacteriophage epsilon15 and its *Salmonella* host during infection. *J. Mol. Biol.* **402,** 731–740
18. Hu, B., Margolin, W., Molineux, I. J., and Liu, J. (2013) The bacteriophage T7 virion undergoes extensive structural remodeling during infection. *Science* **339,** 576–579
19. Silhavy, T. J., Kahne, D., and Walker, S. (2010) The bacterial cell envelope. *Cold Spring Harb. Perspect. Biol.* **2,** a000414
20. Casjens, S. R., and Molineux, I. J. (2012) Short noncontractile tail machines: adsorption and DNA delivery by podoviruses. *Adv. Exp. Med. Biol.* **726,** 143–179
21. Lindberg, A. A. (1973) Bacteriophage receptors. *Annu. Rev. Microbiol.* **27,** 205–241
22. Parent, K. N., Erb, M. L., Cardone, G., Nguyen, K., Gilcrease, E. B., Porcek, N. B., Pogliano, J., Baker, T. S., and Casjens, S. R. (2014) OmpA and OmpC are critical host factors for bacteriophage Sf6 entry in Shigella. *Mol. Microbiol.* **92,** 47–60
23. Zhao, X., Cui, Y., Yan, Y., Du, Z., Tan, Y., Yang, H., Bi, Y., Zhang, P., Zhou,

L., Zhou, D., Han, Y., Song, Y., Wang, X., and Yang, R. (2013) Outer membrane proteins ail and OmpF of *Yersinia pestis* are involved in the adsorption of T7-related bacteriophage Yep-phi. *J. Virol.* **87,** 12260–12269
24. Krüger, D. H., and Schroeder, C. (1981) Bacteriophage T3 and bacteriophage T7 virus-host cell interactions. *Microbiol. Rev.* **45,** 9–51
25. Molineux, I. J. (2001) No syringes please: ejection of phage T7 DNA from the virion is enzyme driven. *Mol. Microbiol.* **40,** 1–8
26. Oliveira, L., Alonso, J. C., and Tavares, P. (2005) A defined *in vitro* system for DNA packaging by the bacteriophage SPP1: insights into the headful packaging mechanism. *J. Mol. Biol.* **353,** 529–539
27. Garcia-Doval, C., and van Raaij, M. J. (2012) Crystallization of the C-terminal domain of the bacteriophage T7 fibre protein gp17. *Acta Crystallogr. Sect. F Struct. Biol. Cryst. Commun.* **68,** 166–171
28. Andres, D., Roske, Y., Doering, C., Heinemann, U., Seckler, R., and Barbirz, S. (2012) Tail morphology controls DNA release in two *Salmonella* phages with one lipopolysaccharide receptor recognition system. *Mol. Microbiol.* **83,** 1244–1253
29. Scheres, S. H., Núñez-Ramírez, R., Sorzano, C. O., Carazo, J. M., and Marabini, R. (2008) Image processing for electron microscopy single-particle analysis using XMIPP. *Nat. Protoc.* **3,** 977–990
30. Sorzano, C. O., Marabini, R., Velázquez-Muriel, J., Bilbao-Castro, J. R., Scheres, S. H., Carazo, J. M., and Pascual-Montano, A. (2004) XMIPP: a new generation of an open-source image processing package for electron microscopy. *J. Struct. Biol.* **148,** 194–204
31. Sorzano, C. O., Bilbao-Castro, J. R., Shkolnisky, Y., Alcorlo, M., Melero, R., Caffarena-Fernández, G., Li, M., Xu, G., Marabini, R., and Carazo, J. M. (2010) A clustering approach to multireference alignment of single-particle projections in electron microscopy. *J. Struct. Biol.* **171,** 197–206
32. Agirrezabala, X., Martín-Benito, J., Castón, J. R., Miranda, R., Valpuesta, J. M., and Carrascosa, J. L. (2005) Maturation of phage T7 involves structural modification of both shell and inner core components. *EMBO J.* **24,** 3820–3829
33. Ludtke, S. J., Baldwin, P. R., and Chiu, W. (1999) EMAN: semiautomated software for high-resolution single-particle reconstructions. *J. Struct. Biol.* **128,** 82–97
34. de la Rosa-Trevín, J. M., Otón, J., Marabini, R., Zaldívar, A., Vargas, J., Carazo, J. M., and Sorzano, C. O. (2013) Xmipp 3.0: an improved software suite for image processing in electron microscopy. *J. Struct. Biol.* **184,** 321–328
35. Pettersen, E. F., Goddard, T. D., Huang, C. C., Couch, G. S., Greenblatt, D. M., Meng, E. C., and Ferrin, T. E. (2004) UCSF Chimera–a visualization system for exploratory research and analysis. *J. Comput. Chem.* **25,** 1605–1612
36. Koike, M., and Iida, K. (1971) Effect of polymyxin on the bacteriophage receptors of the cell walls of Gram-negative bacteria. *J. Bacteriol.* **108,** 1402–1411
37. Andres, D., Hanke, C., Baxa, U., Seul, A., Barbirz, S., and Seckler, R. (2010) Tailspike interactions with lipopolysaccharide effect DNA ejection from phage P22 particles *in vitro*. *J. Biol. Chem.* **285,** 36768–36775
38. Kemp, P., Garcia, L. R., and Molineux, I. J. (2005) Changes in bacteriophage T7 virion structure at the initiation of infection. *Virology* **340,** 307–317
39. Chiaruttini, N., de Frutos, M., Augarde, E., Boulanger, P., Letellier, L., and Viasnoff, V. (2010) Is the *in vitro* ejection of bacteriophage DNA quasistatic? A bulk to single virus study. *Biophys. J.* **99,** 447–455
40. Lhuillier, S., Gallopin, M., Gilquin, B., Brasilès, S., Lancelot, N., Letellier, G., Gilles, M., Dethan, G., Orlova, E. V., Couprie, J., Tavares, P., and Zinn-Justin, S. (2009) Structure of bacteriophage SPP1 head-to-tail connection reveals mechanism for viral DNA gating. *Proc. Natl. Acad. Sci. U.S.A.* **106,** 8507–8512
41. Liu, X., Zhang, Q., Murata, K., Baker, M. L., Sullivan, M. B., Fu, C., Dougherty, M. T., Schmid, M. F., Osburne, M. S., Chisholm, S. W., and Chiu, W. (2010) Structural changes in a marine podovirus associated with release of its genome into *Prochlorococcus*. *Nat. Struct. Mol. Biol.* **17,** 830–836
42. Leiman, P. G., Battisti, A. J., Bowman, V. D., Stummeyer, K., Mühlenhoff, M., Gerardy-Schahn, R., Scholl, D., and Molineux, I. J. (2007) The structures of bacteriophages K1E and K1–5 explain processive degradation of polysaccharide capsules and evolution of new host specificities. *J. Mol. Biol.* **371,** 836–849
43. Jiang, W., Chang, J., Jakana, J., Weigele, P., King, J., and Chiu, W. (2006) Structure of epsilon15 bacteriophage reveals genome organization and DNA packaging/injection apparatus. *Nature* **439,** 612–616
44. Cuervo, A., Chagoyen, M., Pulido-Cid, M., Camacho, A., and Carrascosa, J. L. (2013) Structural characterization of T7 tail machinery reveals a conserved tubular structure among other *Podoviridae* family members and suggests a common mechanism for DNA delivery. *Bacteriophage* 10.4161/bact.27011
45. Qimron, U., Marintcheva, B., Tabor, S., and Richardson, C. C. (2006) Genomewide screens for *Escherichia coli* genes affecting growth of T7 bacteriophage. *Proc. Natl. Acad. Sci. U.S.A.* **103,** 19039–19044
46. Chang, C. Y., Kemp, P., and Molineux, I. J. (2010) gp15 and gp16 cooperate in translocating bacteriophage T7 DNA into the infected cell. *Virology* **398,** 176–186